PASJ: Publ. Astron. Soc. Japan , 1–??, 2011 August 25

Gas Slit Camera (GSC) onboard MAXI on ISS

Tatehiro Mihara, [1] Motoki Nakajima, [2] Mutsumi Sugizaki, [1] Motoko Serino, [1] Masaru Matsuoka, [1] Mitsuhiro Kohama, [3] Kazuyoshi Kawasaki, [3] Hiroshi Tomida, [3] Shiro Ueno, [3] Nobuyuki Kawai, [4] Jun Kataoka, [4] * Mikio Morii, [4] Atsumasa Yoshida, [5] Kazutaka Yamaoka, [5] Satoshi Nakahira, [5] Hitoshi Negoro, [6] Naoki Isobe, [7] Makoto Yamauchi, [8] and Ikuya Sakurai, [1] †

[1] *MAXI team, RIKEN, 2-1 Hirosawa, Wako, Saitama 351-0198*

[2] *School of Dentistry at Matsudo, Nihon University, 2-870-1, Sakaecho-nishi, Matsudo, Chiba 271-8587*

[3] *ISS Science Project Office, ISAS, JAXA, 2-1-1 Sengen, Tsukuba, Ibaraki 305-8505*

[4] *Department of Physics, Tokyo Institute of Technology, 2-12-1 Ookayama, Meguro-ku, Tokyo 152-8551*

[5] *Department of Physics and Mathematics, Aoyama Gakuin University, 5-10-1 Fuchinobe, Sagamihara, Kanagawa 229-8558*

[6] *Department of Physics, Nihon University, 1-8-14, Kanda-Surugadai, Chiyoda-ku, Tokyo 101-8308*

[7] *Department of Astronomy, Kyoto University, Oiwake-cho, Sakyo-ku, Kyoto 606-8502*

[8] *Department of Applied Physics, University of Miyazaki, Gakuen-Kibanadai-Nishi, Miyazaki, Miyazaki 889-2192*

(TM) tmihara@riken.jp

(Received 2011 February 10; accepted 2011 March 22)

Abstract

The Gas Slit Camera (GSC) is an X-ray instrument on the MAXI (Monitor of All-sky X-ray Image) mission on the International Space Station. It is designed to scan the entire sky every 92-minute orbital period in the 2–30 keV band and to achieve the highest sensitivity among the X-ray all-sky monitors ever flown so far. The GSC employs large-area position-sensitive proportional counters with the total detector area of 5350 cm^2. The on-board data processor has functions to format telemetry data as well as to control the high voltage of the proportional counters to protect them from the particle irradiation. The paper describes the instruments, on-board data processing, telemetry data formats, and performance specifications expected from the ground calibration tests.

Key words: instrumentation: detectors – X-rays: general

1. Introduction

All-sky monitors (ASM) have been playing an important role in the research in X-ray astronomy. Since most X-ray sources are highly variable, continuous monitoring of large sky fields and fast acknowledgments of flaring events when they occur are very important for detailed studies with follow-up observations.

The first dedicated ASM, Ariel-V (Holt et al. 1976) observed a number of X-ray novae and transients with two one-dimensional scanning pinhole cameras in 1974–1980. The Ginga satellite operated in 1987–1991 carried an ASM that consists of two proportional counters with six slat collimators rotated by about 16° each (Tsunemi et al. 1989). X-ray novae and transients detected by the ASM were sometimes followed by observations with the main Large Area Counter (LAC) (Turner et al. 1989).

The gamma-ray burst monitors such as Vela-5B (Conner et al. 1969), CGRO/BATSE (Fishman et al. 1993), and Swift/BAT (Gehrels et al. 2004) also work as ASMs. Since 1996, RXTE/ASM has monitored X-ray intensities of hundreds of X-ray sources as well as X-ray novae and transients (Levine et al. 1996). It has three cameras consisting of one-dimensional coded masks and proportional counters. These light curves are open to public through the internet[1] and used by X-ray astronomers world-wide. The long-term data are useful, but the detection limit is about 50 mCrab (5σ) per day. Therefore the targets of RXTE/ASM are mainly on Galactic X-ray sources.

Monitor of All-sky X-ray Image (MAXI) (Matsuoka et al. 2009) is a mission onboard Japanese Experimental Module - Exposed Facility (JEM-EF) on the International Space Station (ISS). It was designed to achieve the better sensitivity than any ASM flown so far using large-area proportional counters with a low background in order to monitor long-term variability of Active Galactic Nuclei (AGN). MAXI carries two kinds of X-ray cameras : Gas Slit Camera (GSC) and Solid-state Slit Camera (SSC: Tsunemi et al. 2010; Tomida et al. 2011). Both GSC and SSC employ slit and collimator optics. The payload was launched by the space shuttle Endevour on July 16, 2009, then mounted on the port No. 1 on JEM-EF on July 24. After the electric power was turned-on on August 3, MAXI started nominal observation since August 15, 2009.

This paper describes the design of the GSC instrument and the expected performance from the ground tests. The in-orbit performance is described in Sugizaki et al. (2011).

* Present Address: Research Institute for Science and Engineering, Waseda University, Shinjuku, Tokyo, 169-8555

† Present Address: Research Center for Synchrotron Radiation, Nagoya University, Nagoya, Aichi, 464-8603

[1] http://xte.mit.edu/ASM_lc.html

2. Camera Design

The MAXI/GSC employs the slit camera optics. The slit camera has an advantage of being free from the source contamination over the coded-aperture mask while it has a disadvantage in the limited slit area. Thus, it is better suited for relatively faint and stable sources such as AGNs. To achieve the high sensitivity, large-area proportional counters filled with Xe gas are used for the X-ray detectors. The total detector area of 5350 cm^2 using twelve gas counters is optimized within the limit of the payload size ($0.8\times1.2\times1.8$ m^3).

Figure 1 illustrates the schematic drawing of the GSC camera units on the MAXI payload. The entire GSC systems are composed of six identical units. Each unit consists of a slit and slat collimator and two proportional counters with one-dimensional position-sensitivity. The two counters in each unit are controlled by two individual data processors (GSC MDP-A/B in section 5) via independent signal paths for the redundancy.

The six camera units are assembled into two groups whose field of views (FOVs) are pointed toward the tangential direction of the ISS motion along the earth horizon and the zenith direction. They are named as horizon and zenith modules respectively. Each horizon/zenith module covers a wide rectangular FOV of $160^\circ\times1.5^\circ$ (FWHM) with an almost equal geometrical area of 10–20 cm^2 combining three camera units. Figure 2 shows the cross-section view of each module. The areas of 10° from the FOV edges to both the rotation poles are not covered because these directions are always obstructed by the ISS structures.

The two FOVs of the horizon and the zenith modules both scan the almost entire sky in the 92 minutes orbital period. Any X-ray source is, therefore, observed twice in a orbit. The horizon module precedes the zenith module by 21.5 minutes in the normal ISS attitude. The FOV of the horizon unit is tilted up by 6 degree above the direction of the ISS motion to avoid the earth atmosphere as an allowance for the possible ISS attitude fluctuation. The FOV of zenith units is set in the plane that includes the zenith and is perpendicular to the direction of motion. Both FOVs have no earth occultation and use no moving mechanics.

In the actual in-orbit operation, observation periods are limited on a low particle-background area in order to protect the counters from the heavy particle irradiation. It reduces the observation duty cycle down to ∼40% (Sugizaki et al. 2011). The two FOVs are capable of covering the whole sky even if some of the counters have to be suspended from operation. The sampling period of 92 minutes is suited to the studies of long-term variability (> 1 hour) such as AGNs.

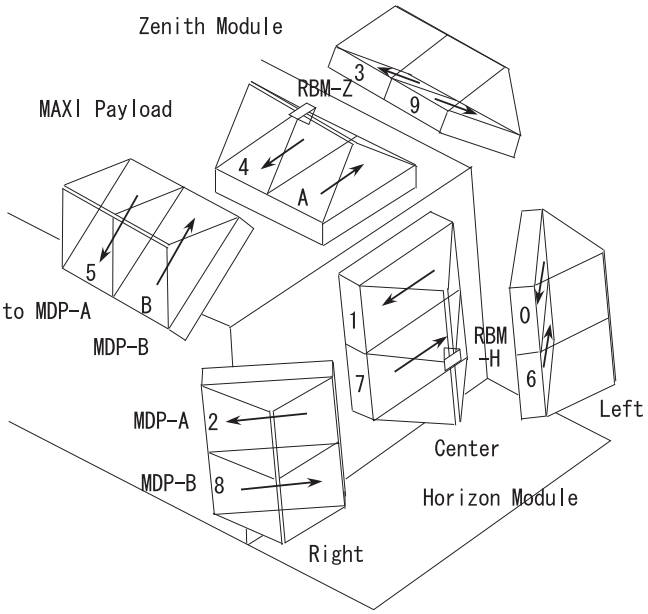

Fig. 1. Schematic drawing of GSC cameras on the MAXI payload. The camera numbers are marked in hexadecimal as 0...9, A and B. Six cameras are assembled into two modules whose field of views are aimed to the horizontal/zenithal directions in orbit. Two cameras in each unit are connected to the two individual readout systems (MDP-A/B) independently for the redundancy. The arrow in each counter indicates the X direction (DETX) of carbon anodes. Two RBM (Radiation-Belt Monitor) detectors are mounted in the middle of the central units of both the horizon and the zenith modules.

3. Detector Unit

3.1. Gas counter

The GSC proportional counters employ resistive carbon fibers with a diameter of 10 μm for anode wires. Higher resistive anodes are preferable for the better position resolution because the thermal noise on the readout signal is inversely proportional to the anode resistance. A carbon fiber is better than a nichrome wire in this point. Although the traditional carbon-coated quartz has a larger resistance, it is mechanically weak, thus easy to break by launch vibration. The carbon fiber anodes in the GSC were developed at RIKEN and were successfully used in the HETE/WXM (Shirasaki et al. 2003).

Figure 3 shows a picture of a single GSC proportional counter. All the flight counters were manufactured by Metorex (now a part of Oxford Instruments) in Finland. The front X-ray window has an area of 192×272 mm^2. It is sealed with a 100-μm-thick beryllium foil. To support the pressure on the beryllium foil in vacuum that amounts 740 kgW in the whole area, grid structures with a 17-mm height are placed every 10.6-mm pitch parallel to the anode wires. The vertical grid is placed only at the center to keep the open area as large as possible. The maximum pressure of 1.66 atm is expected at the temperature of 50°C. Every flight counter was tested to withstand 1.5 times higher than the design pressure, i.e. 2.5 atm. The bodies of the gas counters were made of titanium, which has sufficient strength and a heat expansion coefficient close enough to that of beryllium. The beryllium foil is glued on the body with epoxy.

Figure 4 and 5 show the counter cross-section views.

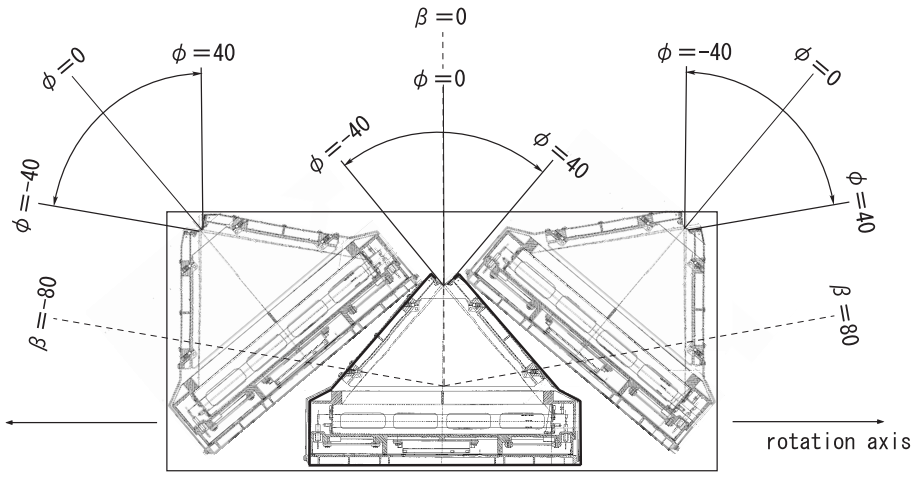

Fig. 2. Cross-section view of each horizon/zenith module. Three camera units are packed in a rectangular space. The incident angle ϕ is defined for each camera, while the source-acquisition angle β is defined for the MAXI payload. The thick outline on the center camera indicates the shields made of 0.1-mm lead and 0.1-mm tin sheets installed to block external X-ray.

The gas cell is divided by ground wires into six carbon-anode cells for X-ray detection and ten tungsten-anode cells for particle veto. The carbon-anode layer and the bottom veto-detector layer have depths of 25 mm and 18 mm, respectively. These sizes are determined so that the main X-ray detectors and the veto detectors have enough efficiencies for X-rays in the 2–30 keV band and minimum-ionization particles, respectively. The minimum-ionization energy in the 18-mm thick Xe gas is 30 keV. The carbon anodes and veto anodes are not located at the center of each cell in the vertical direction. The anode locations, the aspect ratios of these gas cells, and the spacings of the ground wires are determined so that the spatial non-uniformity of gas gain is small within each cell.

The tension of the carbon-anode wire is set to 4 gW, which is sufficiently smaller than the breakage limit, ~ 25 gW. All anode and ground wires are fixed via a spring at right end to absorb the difference of the heat expansion coefficient and keep the wires tight and straight. The veto anode wires are made of gold-coated tungsten with a 18-μm diameter, which is pulled with a tension of 18 gW. We chose as thin wires as possible for veto anodes to achieve similarly high gas gain as the carbon anodes since the same high voltage (HV) is applied to both the carbon anodes and the veto anodes. The gas-gain ratio of carbon anode to the veto anode is 20:1. The ground wires are made of gold-coated tungsten with a 50 μm diameter. The tension is about 50 gW.

We tested several kinds of gas mixture and chose a combination of Xe (99%) + CO_2 (1%) with a pressure of 1.4 atm at 0°C. The amount of CO_2 is decreased from WXM PC (3%) (Shirasaki et al. 2003) in order to reduce the spatial gas-gain non-uniformity (section 8.3), and still keep the sufficient quenching effect (Mihara et al. 2002).

The position resolution and the energy resolution are incompatible requirements. The position resolution is primarily determined by the thermal noise on the resistive-anode wire against the readout signal charge. The higher gas gain is basically preferred for the better position resolution. However, the high voltage for the best position resolution is usually in the limited proportionality region rather than the proportionality range, where the spatial gain non-uniformity is larger due to the space-charge effect, which also degrades the energy resolution. The operating high voltage (HV = 1650 V and the gas gain of 7,000) is chosen to achieve a sufficient position resolution and still keep an adequate energy resolution.

For the in-orbit calibration, a weak radioactive isotope of ^{55}Fe is installed in every counter, which illuminates a small spot of about 1 mm in diameter at the right end of the C2-anode cell (figure 4). Each isotope has a radiation of 30 kBq and its count rate by a GSC counter is about 0.2 c s^{-1} at the launch time.

3.2. Front-end electronics

Each GSC counter has six position-sensitive anodes readout at the both ends (left and right), and two signals for connected veto anodes. A total 14 preamplifiers are used for the 14 analog signals.

The front-end electronics boards are built in the backside of the proportional counter. It is designed to shield external noises and also to strengthen the counter frame. The electronics boards include the high-voltage power supply, HK (House-Keeping) electronics and their connectors. The HK circuit monitors temperatures at eight points in the camera (HV box, preamplifiers, gas cell, etc.) and HV values. The HV-power supply with a low-power consumption was manufactured by Meisei Electric Co. Ltd. Figure 6 illustrates the configuration of the HV connections in each counter. One HV-power-supply unit works on one GSC counter. In total, twelve HV-power-supplies are used. The coupling capacitors connecting the preamplifiers and the anode wires are of 2200 pF, which have sufficiently lower impedance (< 1 kΩ for 2μs shaping out signal of the preamplifier) than that of the

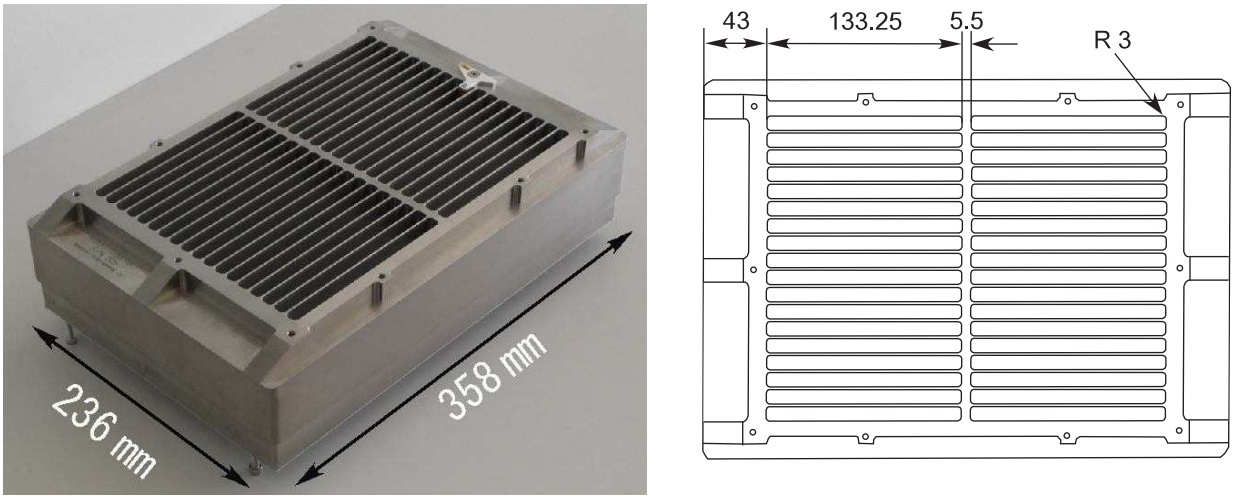

Fig. 3. Proportional counter used in GSC and drawing of the window from the top. See figure 4 and 5 for the cross-section views.
.

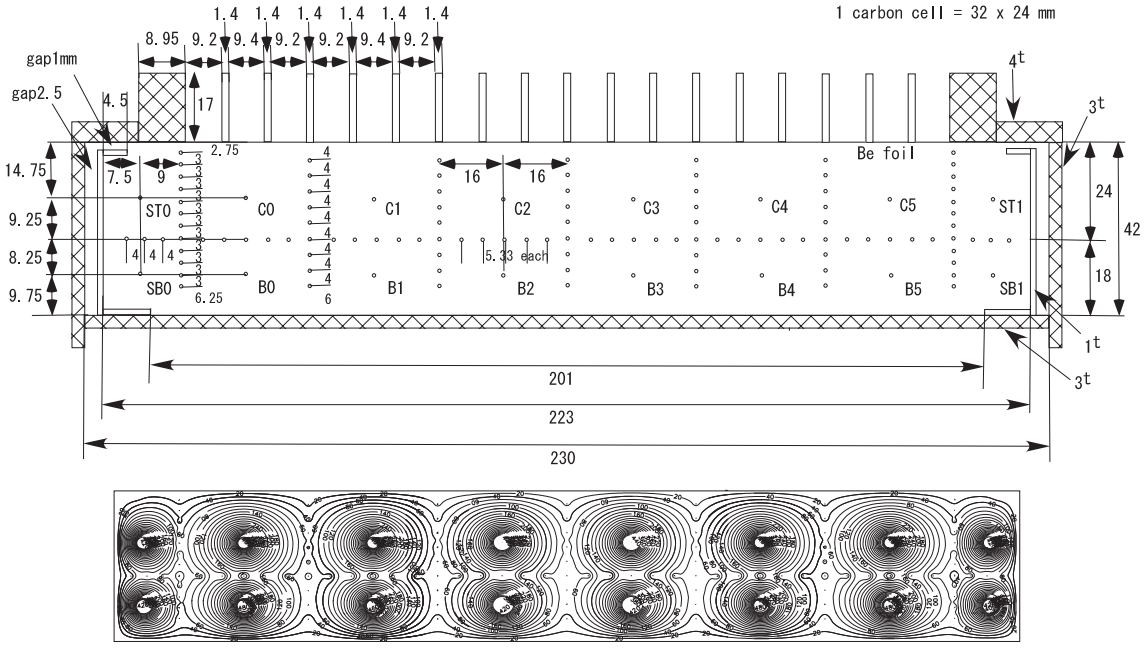

Fig. 4. Cross-section view of GSC proportional counter on the plane perpendicular to the anode wires. All anode/ground-wire locations are shown. The names for anode, C, B, ST and SB, denote Carbon, Bottom, Side Top and Side Bottom, respectively. The wires of B0 to B5 are connected together in the counter and read out as a single bottom-veto (BV) signal. The same for ST0, ST1, SB0 and SB1, as a side-veto (SV) signal. All numbers represent the scale in units of mm. Electric potential in the counter calculated by Garfield is shown in the below. The "Garfield" is a program to simulate gas counters developed in CERN (http://garfield.web.cern.ch/garfield/).

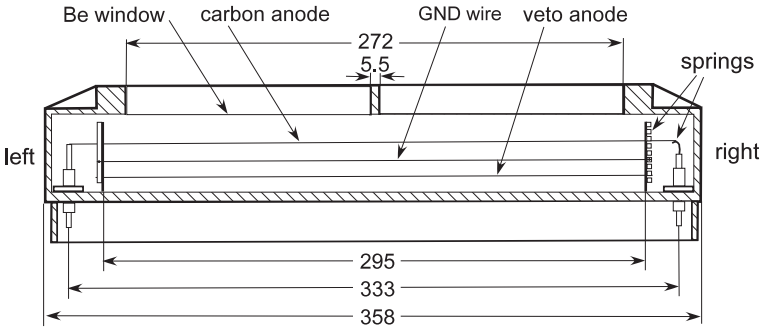

Fig. 5. Cross-section view of GSC proportional counter along the wire direction. Numbers are in units of mm.

carbon anodes (33 kΩ) and still do not accumulate too much charge for the preamplifiers.

Since the wire hermetic rods come out from both the anode ends, two front-end circuit boards are placed separately at the side ends. We selected a hybrid-IC, Amptek A225, for the preamplifier, which is made with a space-use quality and has a low-power consumption.

The preamplifier gains represented by the ratio of the output pulse height to the input charge (Volt/Coulomb) should be the same between the left and the right of each carbon anode. We thus measured gains of all A225 chips under the temperature condition of -20 to 60°C, then selected pairs whose gains show a similar temperature dependence. The feedback capacities of veto anodes are left as they are 1 pF at the default, while those of carbon anodes are modified to 4 pF by adding an external 3 pF capacitor in order to obtain closer pulse heights for both signals from carbon anodes and veto anodes. The ratio becomes 5:1.

3.3. Slit and Slat Collimator

Figure 7 illustrates the schematic view of the GSC slit and slat collimator. The parallel tungsten rods with 3.7-mm separation are placed at the top of the slat collimator constituting the opening slit of the camera. The collimator slats with a 118.4-mm height, placed at 3.1-mm pitch, constitute the FOV of 1.5° in FWHM, which are aligned vertically to the slit rods. The slats are made of phosphor bronze with 0.1 mm thick. The thickness is determined so that X-rays up to 30 keV are stopped and the sheets can be flattened when pulled by the tension springs. These surfaces are chemical-etched and roughened to avoid reflection. 64 slats are installed at the front of each counter. The "roofs" of the collimator module (as shown in a thick outline in Figure 2) and the both ends of slat collimators are covered by 0.1-mm lead and 0.1-mm tin sheets to shield Cosmic X-ray Background (CXB). Twice thicker shield made of 0.3-mm lead and 0.1-mm tin sheets are placed to block the direct path from the space to the beryllium window.

The collimator transmission was tested in the JAXA beam facility. The setup of ground calibration is described in Morii et al. (2006). The transmissions are confirmed to be within ±5 % of the design. A model of the transmission function was constructed based on the measured data. Figure 7 right panel shows a comparison between the measured data and the model. The in-orbit alignment calibration was carried out using celestial X-ray sources, Sco X-1 and the Crab nebula, and is described in Morii et al. (2011).

4. Radiation Belt Monitor (RBM)

The GSC is equipped with RBMs to measure the particle flux which causes background for GSC and SSC, and to protect the instruments from heavy irradiation. Two RBM detectors are mounted at the central part of both the horizon and the zenith modules (figure 1).

Each RBM employs a silicon PIN diode (5×5 mm^2, 200-μm depth) made by Hamamatsu Photonics for its detector. The detector window is covered by a 50-μm-thick aluminum whose particle transmission is equivalent to that of the 100-μm-thick beryllium used for the window of the main proportional counters. The FOV is about $80^\circ \times 50^\circ$. The opening angle of 80° matches the FOV of the central camera unit. The lower-level discriminator (LD) can be set at 4 levels, equivalent to the deposited energies of 30, 50, 200, and 1000 keV. The LD level of 30 keV is sensitive to both electron ($E > 200$ keV) and proton ($E > 2$ MeV). The LD 50 keV is also sensitive for both electrons and protons in the same energies, but efficiency is about 50 % for minimum-ionization particles. The LD 200 keV and 1000 keV are to detect only protons whose energies below 100 MeV and 30 MeV, respectively. The energy losses of electrons and high energy (= minimum-ionization) protons are small and below 200 keV.

The readout electronics are designed to be fast enough to count up to 10^5 c s^{-1}, and do not saturate up to 10^7 c s^{-1}. The count rate limit is high enough so that the RBM can tolerate the in-orbit rate that is expected to be $\sim 10^4$ c s^{-1} in the ISS low-altitude orbit.

The two RBMs, one on horizontal module and the other on the zenithal module, are also considered as the redundancy.[2]

[2] The results obtained in orbit show a slight difference between the two RBMs for the anisotropy of trapped particles, which is reported in another paper for in-orbit performance (Sugizaki et al. 2011).

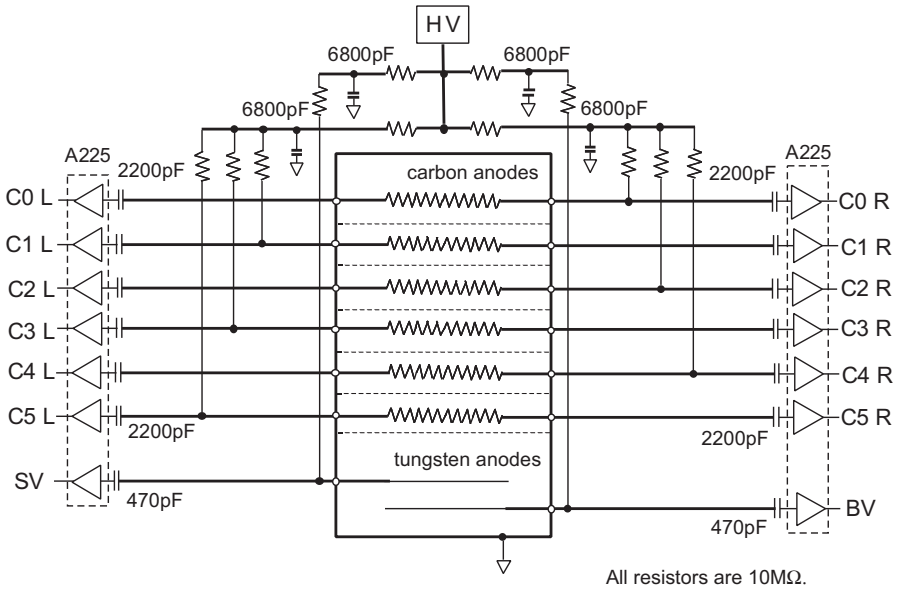

Fig. 6. Schematic view of high-voltage connections to anode wires on the front-end circuit board.

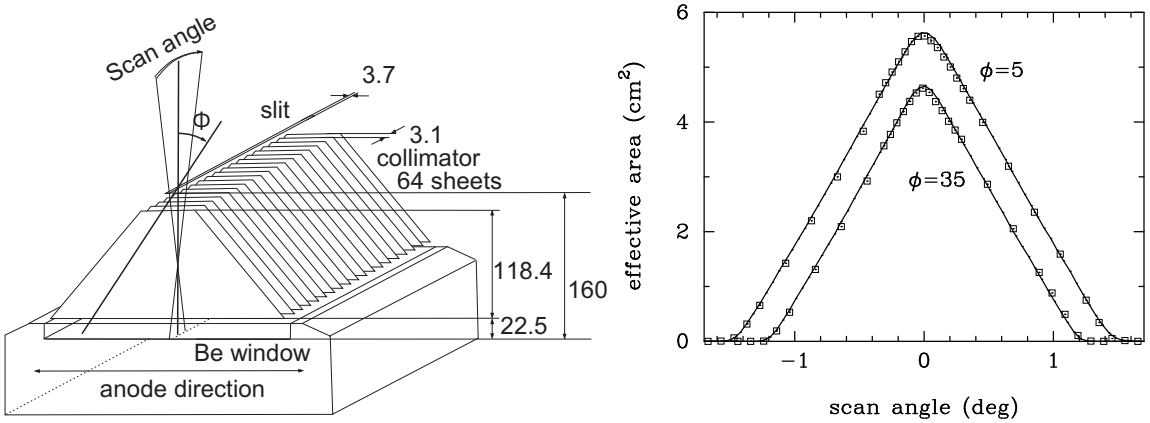

Fig. 7. (Left): Geometry of GSC slit and slat collimator. All numbers represent the scales in units of mm. Collimator sheets are 0.1-mm thick and placed by 3.1-mm pitch. (Right): Effective area of slit and slat collimator for $\phi = 5°$, $35°$. Points represent data measured with X-rays at Cu-K line (8.0 keV) in a ground test and solid lines represent the response models constructed for the data.

5. On-board Data Processing System

5.1. Mission Data Processor (MDP)

The GSC electronics system, named GSC Mission Data Processor (MDP, hereafter), processes a total of 168-channel analog signals from 12 position-sensitive proportional counters. It also have a function to manipulates the readout event data and to receive and process commands from the central MAXI data processor (DP). Figure 8 illustrates the block diagram of the MDP data processing. The system consists of two identical modules (MDP-A and MDP-B) for the redundancy. Each MDP consists of six analog boards and one digital board to process signals of six counters, a half of the entire twelve counters. Each analog board embodies circuits to process signals from one counter.

We developed a hybrid IC for the GSC analog signal processing, which is named HIC-MAXI. One HIC-MAXI package contains a gain amplifier, a shaping amplifier, an LD and a peak hold circuit for a single analog channel. Each analog board carries 14 packages. The gain and LD are adjustable by command to 512 levels ($\times 1.0 - 36.0$, nominal 5.0) and 4 levels (typically equivalent to the X-ray energies of 0.25, 0.5, 1.0, 2.0 keV, nominal 1.0 keV), respectively. The design of the shaping amplifier is optimized for the counter position resolution. It consists of one-order high-pass filter with a cutoff at 145 kHz and two-order low-pass filter at 2.1 MHz. The peak-hold capacitor of 1000 pF is chosen to sharpen the LD-cut threshold. Since a MOS FET, SD215, used to discharge the peak-hold capacitor was found to be weak for heavy irradiation, it were replaced by the radiation-tolerant version fabricated by Calogics. Furthermore, the HIC package

was shielded with a 2-mm-thick iron. It then accepts the total dose requirement of 2.8 krad (for 2 years, including the safety factor of 3). All other electric parts have a specification of the radiation hardness tolerant for 10 krad.

Each analog board embodies a 14-bit ADC, AD 7899, whose conversion time is 2μs. While 8-bit precision is sufficient for the energy resolution of the proportional counter, a 14-bit ADC is required for obtaining a positional value with a precision of ~ 0.1 mm precision along the 333 mm anode wire even for small pulse-height events.

The position along the anode wire is encoded into the ratio of two PHAs (Pulse Height Amplitudes) read out at the both ends. Fourteen channels in each counter are processed by a single ADC. Each signal is peak-held, then is fed to the ADC one by one through a multiplexer.

The digital processing was programmed on the fuse-type FPGAs operated at 10-MHz clock frequency, fabricated by ACTEL. They are used on both the analog and digital boards.

5.2. Event-data processing

The front-end data processing is started when a LD-hit signal is issued at any of 14 signal channels. It triggers the peak-holds of all the 14 analog outputs in each counter. The coincidence of the 14 LD-hit signals is judged within the 10-μs window. The readout process is activated if the coincidence satisfies the required combination. The hit-patterns of the readout events can be changed by commanding. In the nominal configuration, only those events in which the LD-hit signal is found only from a single carbon anode are processed.

The GSC has two event-readout modes: one is the observation mode and the other is diagnostic mode. In the normal observation mode, two PHA data from a carbon anode with LD hits are A/D converted, then processed into the telemetry data. In the diagnostic mode, all the 14 signals are processed. The A/D conversion takes 20 μs for two PHA data in the observation mode and 140 μs for 14 PHA data in the diagnostic mode. The dead time for the analog processing becomes about 30 μs and 150 μs in observation and diagnostic modes, respectively. The diagnostic mode are used for the detector health check.

The LD-hit count in each anode is always monitored by LD-hit counters. These count data are stored in the HK data in the telemetry every second. The counter data also includes information of multiple hits (the numbers of carbon-carbon or veto-carbon coincidences). The hardware upper-level discriminator is not equipped on the circuit board. Instead, the rate of events whose pulse height at either end is saturated in A/D conversion are monitored.

5.3. Event Timing

Each MDP-A/B system is equipped with a 20-kHz free-run clock counter (FRC) with a 16-bit length to measure each event time with a 50-μs precision. When the event-readout process is activated by a LD-hit signal, the number of the FRC is latched and included into the event data.

Each event data in the telemetry has a time tag of DP clock counter (DPTC) that is incremented every second. The timing of the DPTC and FRCs on GSC MDP-A/B systems can be calibrated on the ground using data of an on-board GPS which are also downloaded through the telemetry.

6. Telemetry Data

6.1. DP Event Data Reduction

The MAXI Data Processor (DP) employs a multi-CPU computer system using MIPS R3081. The DP controls all payload instruments including GSC by real-time and scheduled commands. It also packages the telemetry data to be downlinked to the ground.

The DP receives GSC event data from the GSC MDP-A/B via RS-422 connection. Each MDP can transfer 2,000 event data every second at the maximum. The data rate corresponds to 285 events s^{-1} in the diagnostic mode.

The event data are usually reduced in units of the 64-bit format which consists of an camera number (4 bits) an anode ID number (4 bits), two pulse height data (14 bits $\times$2) at the both anode ends (Left and Right), value of the 20-kHz clock counter at event timing (16 bits), hit pattern of the 14 gas-counter signals (both ends of six carbon anodes and two sets of veto-counter signals) (8 bits), and data-readout mode (observation/diagnostic) (4 bits). The telemetry formatting occurs every second. In the observation mode, each single-event data consists of the 64-bit-format units. In the diagnostic mode, each event consists of seven 64-bit units; six for the six carbon-anodes and one for the two veto anodes.

Since the telemetry bandwidth between the ISS and the ground is limited, there are options to reduce the data mass. The DP has a function to filter event data with the software LD and UD, which can be set separately for the two downlink paths (MIL-1553B and ethernet; see the next subsection), in each counter. The telemetry event data also have three reduction modes: 64-bit, 32-bit and 16-bit to be able to fit the limited data rate. In the 64 bit mode, the primary 64-bit-format data are transferred without any reduction. In the 32 bit mode, each 64-bit data are reduced to 32 bits which consists of camera number (3 bits), anode number (3 bits), two PHAs (13 bits $\times$ 2). In the 16 bit mode, camera number (3 bits), pre-registered encoded numbers for position (eg. 8 bits) and energy (eg. 5 bits) are returned. The bit assignments in 16 bit mode are commandable. Table 1 summarizes the bit assignments of the three telemetry-reduction modes. [3]

6.2. Data Downlink Flows and Bandwidth

MAXI has two data downlink paths to the ground, the MIL-STD-1553B (MIL-1553B hereafter) and the ethernet,

[3] Prior to the MAXI launch the nominal data-reduction mode for MIL-1553B downlink was set to the 32-bit mode, which continued for the initial operation phase. It was changed to the 64-bit mode on October 30, 2009. The data through the ethernet downlink always takes the 64 bit mode.

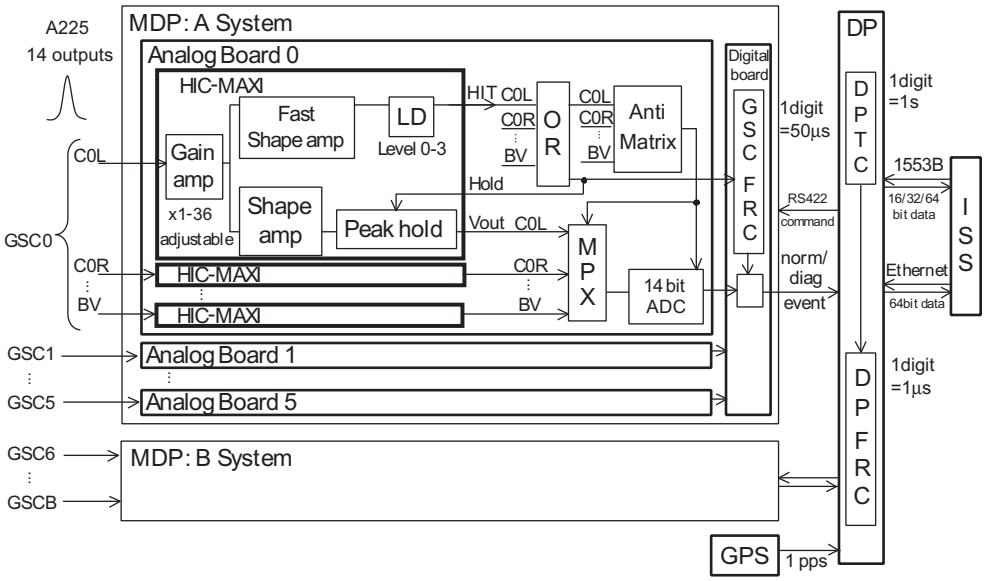

Fig. 8. Block diagram of event-data readout flows on the GSC Mission Data Processor (MDP).

Table 1. Bit assignments of event data in three telemetry-reduction mode

Reduction Mode	GSCID	ANODE	PHA	GSC-FRC	HIT-PTRN	MODE
64-bit	4	4	14×2	16	8	4
32-bit	3	3	13×2	0	0	0
16-bit	3	0	8* (position) + 5* (energy)	0	0	0

*: The bit assignment between position and energy data are commandable within the total 13 bits.

whose maximum data-transfer rates are 51 kbps and 600 kbps, respectively. While the ethernet has an advantage in the speed, the MIL-1553B is superior in the connection reliability. GSC usually uses 50 kbps of the ethernet and SSC 200 kbps. SSC mainly uses the ethernet for the event data.

GSC can use about 70% of the MIL-1553B bandwidth assigned to MAXI. If the event rate exceeds the limit, the overflow data are stored in the DP buffer. The buffered data are transferred later when the data rate becomes lower than the limit. The buffer for each of two readout systems (A/B) has a volume of 500 kByte and can store 62,000 events in the 64-bit format. The buffer data should keep the data for 50 seconds typically, which corresponds to the single-scan duration of a point source. Since the expected event rate for the Crab nebula is 31 events s^{-1} for each system, bright sources with up to 40 Crab fluxes can be observed without any data loss in the 64bit mode. Note that the brightest X-ray source, Sco X-1, is about 16 Crab in 2–20 keV.

7. Detector protection

The proportional counter must be operated carefully in orbit not to suffer from any breakdown. GSC has various protection functions in hardware and software to avoid undesirably high count rates. The MDP equips a hardware protection function using RBM counter. The DP has four kinds of protections in software using information of RBM counts, location of ISS, location of the sun, and the LD count rates.

7.1. On-board RBM Protection

A protection function using the RBM count rates is implemented in the MDP circuit. When either count rate of the two RBMs exceeds the threshold, HVs of all the twelve counters are reduced to 0 V. The threshold of each RBM can be changed individually by commanding. The HV suppression is released when the count becomes less than the half of the threshold. These judgments are made every 10 seconds. [4]

7.2. DP Software Protection

The DP software can perform more flexible and finer controls of the counter HVs using information collected from all the subsystems. The DP is always monitoring the parameters relevant to the counter protections described in the following subsections and reduces the HVs of the related gas counters to 0 V when any of the parameters reaches the threshold. The HV suppression is released automatically when they are recognized to return to the normal condition. The DP slowly raises the HV not to

[4] The thresholds for both horizon and zenith RBMs are set at 100 counts in 10 seconds in the flight operation . The MDP-RBM flag is high during about 11 % of the whole time, and in 3 % of the low-lattitude time.

stress the counters. The nominal rate is an increment with a 330-V step every 10 second, which can be changed by commanding for each counter.

7.2.1. RBM-Count Protection

The DP also offers a protection with RBM, but in a more sophisticated manner than that by the hardware as described in section 7.1. The accumulation of the RBM counts and its judgement are carried out every second in the sliding window. The threshold level and the accumulation period (nominal 20 seconds) are commandable. The criteria for the HV reduction and the recovery are the same as the hardware one. When either of the integrated counts of the two RBMs exceeds their threshold, the HVs of all the 12 counters are reduced to 0 V. The HV suppression is released when both the integrated counts become less than the halves of their thresholds.

7.2.2. Radiation-Zone Protection

The Radiation-Zone (RZ) protection is designed to avoid particle irradiation predicted from the geographical location such as SAA. DP keeps three RZ-map data with $2.5^\circ \times 2.5^\circ$ mesh for three different altitudes. When ISS enters a radiation area defined by the RZ maps, the HVs of all the 12 counters are reduced to 0 V. The ISS location are obtained from the ISS ancillary data, which are broadcasted on the ISS common network of MIL-1553B.

7.2.3. Sun Protection

Since GSC scans the almost entire sky every orbital cycle, the direction to the sun is also covered by some GSC camera units. The Sun protection is designed to avoid a direct sun illumination on the detector, where unfavorable high count rates area expected. The direction to the sun is calculated using the ISS ancillary data. If the sun is closer to the FOVs of some camera units than the limit, the HVs of these cameras are reduced to 0 V. The limit of the separation between the sun direction and the camera FOV can be changed by commands.[5]

7.2.4. LD-Count Protection

Every anode signal of each camera has a LD-hit counter (subsection 5.1). The LD-count protection is designed to avoid damages by any unexpected high count rates such as breakdown. Two kinds of counting methods are implemented to be sensitive to various break modes on the detector.

1. Integrated High Flag
   If a breakdown occurs, the count-rate suddenly increases to a high level. Every second, DP calculates the integrated number of LD-hit counts of all anodes in a camera during a given period. If it exceeds the threshold, the high voltage of the counter is reduced to 0 V. The integration is done by the sliding window.
2. Continuous High Flag
   If a moderate spark occurs, the count-rate becomes slightly high continuously. In such a case the continuous high flag works. If a total LD-hit count of all anodes stays over the threshold for a given period, the high voltage of the camera is reduced to 0 V.

These thresholds can be set for each counter individually by commanding. In these LD-count protection, the HV suppression is released after a 5-minute wait time.[6]

8. Detector performance

8.1. Energy Band and Efficiency

The efficiency curve is shown in figure 5 in Matsuoka et al. (2009). It stays higher than 15% in the GSC nominal energy range of 2–30 keV. In the lower energy end, the efficiency drops due to the absorption in the 100-μm-thick beryllium window and varies from 2 to 5% at 1.5 keV according to the X-ray incident angle of 0°–40°. In the higher energy range, the efficiency jumps up at the Xe K-edge energy of 34.6 keV by a factor of 4.8. X-ray events whose energy is higher than the K-edge lose K-line energy due to the escape of fluorescence lines. The escape probability of Xe K-line is 66%, thus it has a significant effect on the counter response. We measured the escape fraction and the complex energy response around the Xe K-edge energy using GSC flight-spare counter at KEK photon factory[7].

8.2. Energy response

The GSC gas counter is operated at the nominal HV of 1650V, which is chosen to achieve a good position resolution. It is in the limited proportionality region where the energy-PHA relation is rather distorted. Thus, the detail calibration is necessary to construct the energy-PHA response matrix. The tests for the energy response calibration were carried out for all the flight counters using X-ray beams including fluorescence lines from various target elements placed in the X-ray generator. Figure 9 shows the obtained typical energy spectra.

Figure 10 shows the energy-PHA relation derived from the calibration-test data. It has a discontinuity at 4.7 keV for Xe L-edge. The relation is well reproduced by two expedient functions for those below and above the L-edge. The deviations between the data and the model functions are within 0.6% over the 2–23 keV band.

Figure 11 shows the obtained energy resolution against the X-ray energy and that of the theoretical limit. The measured energy resolution is 16 % (FWHM) at 6 keV. It is close to the theoretical limit in the 3–5 keV band. The difference is larger at low and high energies. At low energies, a part of the electron cloud is lost by the beryllium window. At high energies, the spatial gain non-uniformity becomes effective according to the large mean free path.

[5] The limit of the sun angle has been reduced from 30° at the initial operation to 4° in the nominal operation to optimize the sky coverage.

[6] On April 18, 2010, the ISS auxiliary data was stopped due to the ISS computer trouble, and the sun went into the FOV of a GSC camera. The integrated high flag became on and the HV of the camera was shutdown safely. At that time the sun reached one-fourth to the center of FOV. The flux of the sun was measured 1400 Crab in 2-4 keV.

[7] http://www.kek.jp/intra-e/research/PF.html

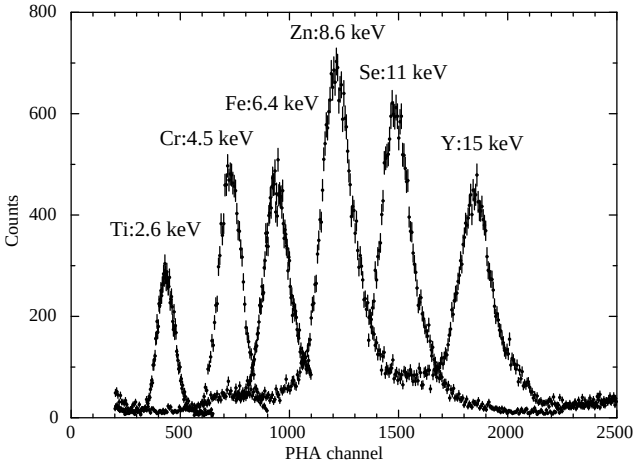

Fig. 9. Energy spectra for K-shell emission lines from Ti (2.4 keV), Cr (4.5 keV), Fe (6.4 kV), Zn (8.6 keV), Se (11 keV), and Y (15 keV). The data were taken for pencil X-ray beams irradiated at an off-wire position of counter #0 anode C0 in the nominal anode HV of 1650 V.

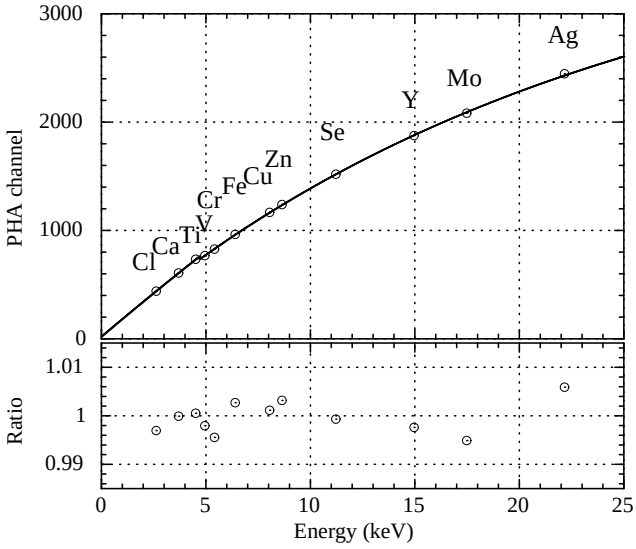

Fig. 10. Linearity of energy-PHA (Pulse height amplitude) relation. Circles represent measured data for K-shell emission lines from the elements labeled. The data were taken in the same condition with those of figure 9. Bottom panel shows residuals from a model expressed by expedient function, $a - b\exp(cE)$. The discontinuity at the Xe L-edge (4.70 keV) is implemented in the model.

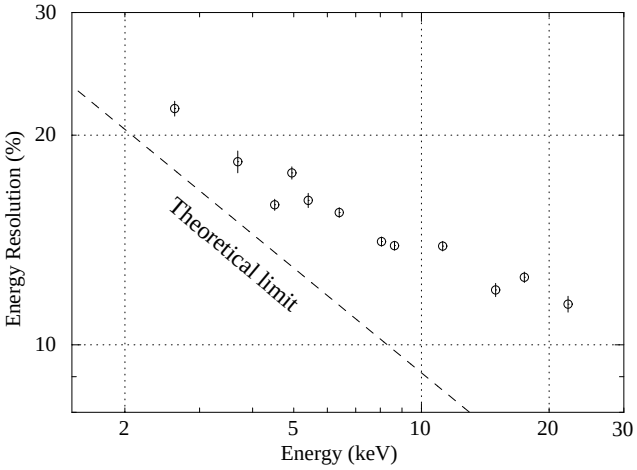

Fig. 11. Energy resolution (FWHM) against X-ray energy. Circles with 1-σ error bars represent measured data with K-shell emission lines from the elements same as those in figure 10. The theoretical limit is estimated as $2.35\{W(F+b)/E\}^{1/2}$, where the mean ionization energy $W = 21.5$ eV, the Fano-factor $F = 0.2$, and dispersion of gas gain in electron avalanche $b = 0.5$ are assumed (Knoll 1989).

8.3. Gain Spatial Non-uniformity

The gain non-uniformity along the anode wire is measured with a 2 mm pitch using Cu K_α (8.0 keV) and Mo K_α (17.5 keV) X-ray beams with a diameter of 0.2 mm. The non-uniformity among each anode cell is ~ 20 % typically. The data is used in the PHA-PI conversion carried out on the ground data reduction and also to build the energy response matrix in the spectral analysis.

The non-uniformity on the vertical plane to the anode wire was measured with slant X-ray beams taking an advantage of the position sensitivity. The method is described in Mihara et al. (2002). Figure 12 shows the obtained gain non-uniformity around the anode wire. The gain is the highest in the annulus of an about 5-mm radius from the anode. It is lower than the average at the central region around the anode wire and the outer region. Compared to the distribution of the electric potential in figure 4, the gain has a positive correlation with the field strength in the outer region.

8.4. Position Response

Since the GSC employs slit-camera optics, the detector position response is important for determining the direction of incident X-ray photons with a good accuracy. The data of the position response is taken with a 1-mm pitch along the carbon anode using X-ray beams of Cu K-line in the ground calibration tests.

The position is encoded in the ratio of the pulse height readouts at the both anode ends. We here define the two PHA as the left $PHA_{\rm L}$ and the right $PHA_{\rm R}$ and introduce a position-measure parameter, PM,

$$PM = \frac{PHA_{\rm R} - PHA_{\rm L}}{PHA_{\rm R} + PHA_{\rm L}} \quad (1)$$

The position-measure parameter has an approximately

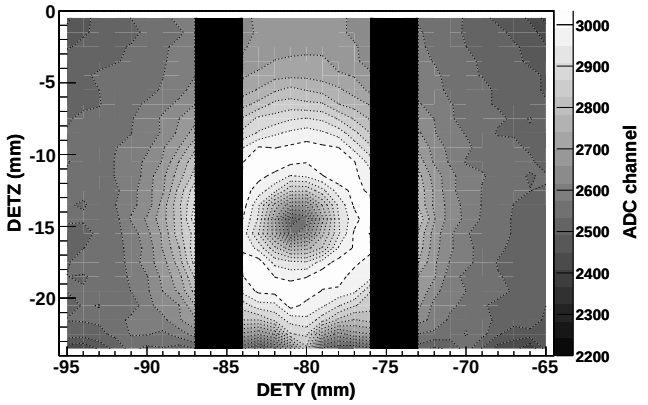

Fig. 12. Cross section of gas-gain non-uniformity in a single carbon-anode cell (C0 cell) on the plane perpendicular to the anode wire. The DETY direction is parallel to the detector window and the DETZ represent the depth from the the beryllium-window plane. The anode position is $(-80, -14.75)$. The data are obtained by the slant-beam method using X-ray beams of Mo K-line (17.5 keV). Two black stripes are unmeasurable region located under the counter-support structure. The gray scale represents the the pulse heights of the output signals for the Mo K-line.

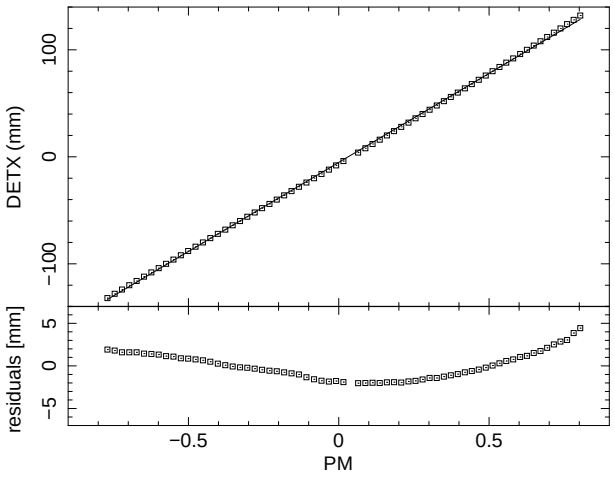

Fig. 13. Relation between the position at which X-ray is absorbed along the anode wire (DETX) and the position-measure parameter derived from the PHA ratio (PM : see text). This is for the GSC camera 6, anode 0 measured at the nominal HV of 1650 V using pencil X-ray beam of Cu K_α line . The data (square) are fitted with a linear function (solid line) in the top panel, and the residuals are shown in the bottom panel.

linear relation with the event location where the X-ray is absorbed along the anode wire (figure 13). However, the relation cannot be exactly linear in the real experiment. Any analytic function cannot successfully reproduce the data obtained in the calibration tests with the required position accuracy. We thus decided to use the table-lookup method in the response function based on the ground calibration tests.

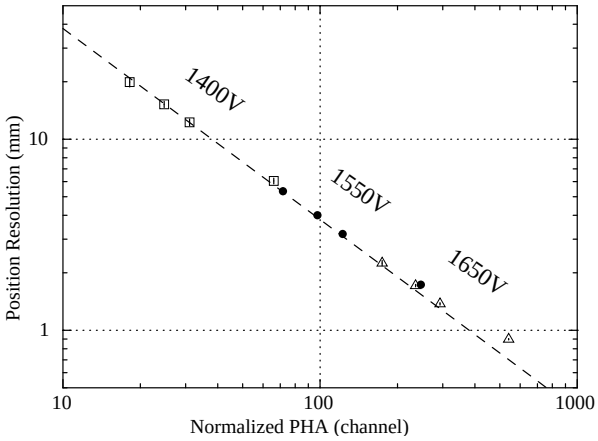

Fig. 14. Relation between position resolution (FWHM) and signal pulse height normalized by read-out amplifier gain. Squares, filled circle, and triangle points are data taken at the HV of 1400 V, 1550 V, and 1650 V, respectively. Four data points at each HV are the resolutions for Ti-K_α+K_β (4.5 keV), Fe-K_α (6.4 keV), Cu-K_α (8.0 keV) and Mo-K_α (17.5 keV). The dashed line represents an inversely proportional relation.

8.5. Position Resolution and High Voltage

The position resolution should be better than the slit opening width of 3.7mm to achieve the optimal angular resolution. It is mostly determined by the ratio of the thermal noise to signal charges, which are the photoelectrons multiplied by the avalanche process in the counter.

Figure 14 shows the relation between the measured position resolution and the signal pulse height normalized by the readout-amplifier gain, obtained from data taken for X-ray beams of Ti-K_α+K_β (4.5 keV), Fe-K_α (6.4 keV), Cu-K_α (8.0 keV) and Mo-K_α (17.5 keV) in three anode voltages of 1400, 1550 and 1650 V. It is clear that the position resolution is inversely proportional to the pulse height. It is because the equivalent noise charge is constant in each anode and the position resolution depends only on the number of the multiplied signal charges. The rightmost point, measured for Mo-K_α at 1650 V, is slightly higher than the line because the mean free path of the photoelectron (~ 0.5 mm for 17.5 keV) is not negligible (Tabata et al. 1972).

We determined the nominal anode voltage of 1650 V based on the results.

8.6. Anti-coincidence

Figure 15 shows energy spectra and count-rate distributions of the room background events. Those with and without anti-coincidence cut are shown. The energy band of 2–30 keV is used for the plot. The data are obtained as a part of the final ground tests at Kennedy Space center in 2008 November. The background rate at KSC was about 90 % of that in Tsukuba Space Center. The anti-coincidence cut reduces the event rate down to about 1/9. The remaining room background rate is 1.0×10^{-4} c s^{-1} cm^{-2} keV^{-1} in 2–30 keV. The room background mainly consists of gamma rays such as ^{40}K. The spectrum shape

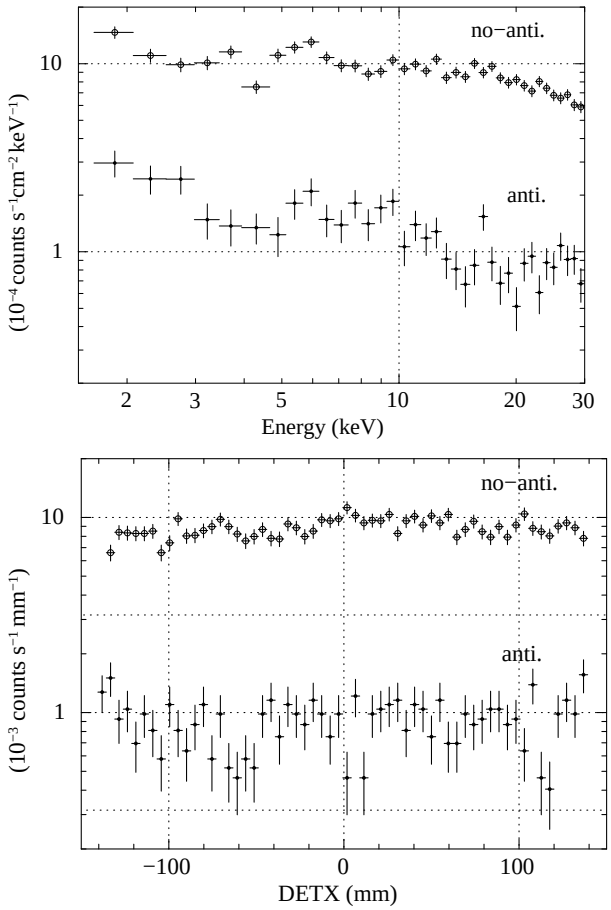

Fig. 15. Energy spectra (top) and position distributions along the anode (DETX) (bottom) of the room background taken in the final ground test at Kennedy Space center in 2008 November. The measurements for counter #0 anode C0 taken with and without anti-coincidence cut, are shown . The anode-cell length in the DETX direction is −136 to +136 mm and the width is 32 mm.

does not change with and without the anti-coincidence.

9. Summary

The GSC is one of the X-ray instruments of the MAXI mission on the ISS. It is designed to scan the entire sky every 92-minute orbital period in the 2–30 keV band and to achieve the highest sensitivity among the all-sky X-ray monitors built so far. It employs large-area position-sensitive proportional counters with a total detector area of 5350 cm^2 and the slit and slat collimators defining two rectangular FOVs of 1.5°(FWHM)×160° to optimize the monitoring of relatively faint sources including AGNs. The on-board data processor (DP) has functions to format telemetry data for the two download paths different in the bandwidth and to protect the gas counters from particle irradiation in orbit. The ground calibration tests confirmed the effective area in the energy band of 2–30 keV, the energy resolution of 16% (FWHM) at 6 keV, the energy response in the limited proportionality region, the spatial non-uniformity of gas gain about 20%, the detector position resolution of 1–4 mm varying with X-ray energy at the nominal HV of 1650 V, and the background rejection efficiency by the anti-coincidence technique.

Authors thank Metorex (Oxford Instrument), Meisei Electric Co. Ltd., and NEC Co. Ltd., in particular to Matti Kaipiainen for the development and fabrication of the GSC proportional counters, Isao Tanaka, Nobuyuki Kidachi, Koji Taguchi for the development and production of the collimators and the electronics, and Takahiko Tanaka, Hiroshi Mondo for the development of the DP. This research was partially supported by the Ministry of Education, Culture, Sports, Science and Technology (MEXT), Grant-in-Aid for Science Research 19047001, 20244015, 21340043, 21740140, 22740120 and Global- COE from MEXT "Nanoscience and Quantum Physics" and "The Next Generation of Physics, Spun from Universality and Emergence".

References

Conner, J. P., Evans, W. D., & Belian, R. D. 1969, ApJL, 157, L157
Fishman, G. J., et al. 1993, A&AS, 97, 17
Gehrels, N., et al. 2004, ApJ, 611, 1005
Holt, S. S., et al. 1976, Ap&SS, 42, 123
Knoll, G. F. 1989, Radiation Detection and Measurement (Second edition) John Wiley & Sons, Inc.
Levine, A. M., Bradt, H., Cui, W., Jernigan, J. G., et al. 1996, ApJ, 469, L33
Matsuoka, M. et al. 2009, PASJ, 61, 999
Mihara, T., et al., 2002, Proc. SPIE, 4497, 173
Morii, M., Sugimori, K., & Kawai, N. 2011, Physica E: Low-dimensional Systems and Nanostructures, 43, 692
Morii, M., et al., 2006, in Space Telescope and Instr. II ed. Turner, M. J. L. & Hasinger, G. Proc. SPIE, 6266, 6263U.
Shirasaki, Y., et al. 2003, PASJ, 55, 1033
Sugizaki, M., et al. 2011, PASJ, in print.
Tabata, T., et al. 1972, NIMM, 103, 85
Tomida, H., et al. 2011, PASJ, in print.
Tsunemi, H., Kitamoto, S., Manabe, M., Miyamoto, S., Yamashita, K., & Nakagawa, M. 1989, PASJ, 41, 391
Tsunemi, H., Tomida, H., Katayama, H., Kimura, M., Daikyuji, A., Miyaguchi, K., Maeda, K., & MAXI Team. 2010, PASJ, 62, 1371
Turner, M. J. L., et al. 1989, PASJ, 41, 345